Proceedings of the 2003 IEEE
International Conference on Robotics & Automation
Taipei, Taiwan, September 14-19, 2003

A Thermally Actuated Polymer Micro Robotic Gripper for Manipulation of Biological Cells

Ho-Yin Chan[1] and Wen J. Li[1,2,*,+]

[1]Centre for Micro and Nano Systems, The Chinese University of Hong Kong, Shatin, N.T., Hong Kong SAR
[2]Robotics Laboratory, Shenyang Institute of Automation, Chinese Academy of Sciences, Shenyang, China

*Contacting Author: wen@acae.cuhk.edu.hk

Abstract **- The development of a novel polymer-based micro robotic gripper that can be actuated in a liquid medium is presented in this paper. The basic structure for the gripper is a trimorph thermal actuator with a platinum metal heater encapsulated by poly-para-xylylene C (parylene C) polymer layers. Due to the large difference of thermal expansion coefficients of the different layers, the actuator can be actuated with much large deflection than conventional MEMS actuators. We have developed actuators operating in liquid environment (e.g., DI water) with only 3V at ~33mA input to achieve full deflection (90° change of tip direction). The actuators were also observed to respond to 3Hz square wave input in water with no visible delay. The temperature of the actuators at full deflection was estimated to be about 60°C, which is much lower than the typical requirement of >100°C to actuate other conventional MEMS actuators. Actuators with dimensions of ~2mmx100μmx0.6μm were used to capture *Danio rerio* follicles (~800μm average cell diameter) in water. The design, fabrication process, and experimental results for these actuators are presented in this paper.**

I. INTRODUCTION

Potential applications for microrobotics with growing interest are cell manipulation, cell isolation, and micro injection (e.g., see [1]). For example, biologists usually use pipettes for cell isolation prior to carrying out micro injection. However, the functionality of this method is limited by the size of the cells, i.e., the cells cannot be too small compared to the pipette; otherwise, a bundle of cells could be drawn into the pipette at once. In addition, the pipette cannot be used to rotate individual cells, a function which is highly desirable during a micro injection process. To address these problems, we are currently developing an on-chip microrobotic gripper system that can eventually be used to manipulate and isolate cells controllably, and that can potentially be used to conduct localized cell probing and measurement. We report in this paper a novel micro polymer-based actuator that can be configured to form single-finger for multiple-finger underwater robotic grippers for cell grasping. Our group has also recently developed a nanometer scale "nano-cutter" [2] to be used for cell probing and cutting. By combining these technologies, micro cellular surgery may become feasible in the near future (see conceptual illustration in Fig. 1).

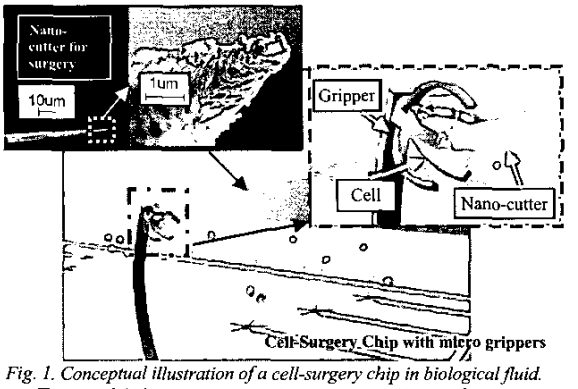

Fig. 1. Conceptual illustration of a cell-surgery chip in biological fluid. The inset SEM picture is a sample nano-cutter fabricated in our laboratory which can be potentially used for cell-surgery [2].

Although many MEMS actuators exist already they are all hindered by one or more of the following factors when actuation in biological fluids is required: small displacement, small force output, large power consumption, large voltage requirement, and bio-incompatibility. For example, electrostatic actuators are inefficient in ion-rich fluid and their deflection is very small [3]. Therefore, thermal actuators were considered by some researchers to operate in solution-based environments. Thermal actuators generally consist two structural layers with different thermal expansion coefficients ("bimorph"). One of the layers would be used as a heater to generate heat to induce thermal expansion of the two layers. Due to mismatch of the thermally-induced strain, the structure could be made to bend as a function of the heat generated. Even though thermal actuators can produce larger force and deflection than other types of MEMS actuators, they require higher power to actuate. G. Lin et al. [4] demonstrated a 2-layer thermal actuator (200μm × 45μm × 1.1μm with polyimide/Au layers) that can operate in air with 7V at 4mA. However, to operate in liquid, it required over 100V to actuate and overheated the actuator. M. Ataka et al. [5] also fabricated a thermal bimorph actuator (500μm × 100μm × 6μm with polyimide/Au layers) which rose up to 260°C for actuation in water – a temperature that would definitely kill cells. Recently, researchers have begun to look into other materials and mechanisms for underwater actuation. For example,

* Wen J. Li is an associate professor at the Chinese University of Hong Kong and also serving as an affiliated professor at the Shenyang Institute of Automation. This project is funded by the Hong Kong Research Grants Council (CUHK4206/00E) and by the Chinese Academy of Sciences' Distinguished Overseas Scholar Grant.

Jager et al. [6] and Smela et al. [7] have pioneered the usage of polypyrrole polymers to fabricate micro aqueous actuators that can be driven under 2V. However, their actuators are limited to operation in electrolyte solutions, which are not suitable for the survival of many biological entities.

Our ongoing work is to use parylene C as a thin film polymer to encapsulate a thin film metal heater, resulting in a tri-layered thermal actuator. Parylene C is bio-compatible, has excellent thermal and electrical insulation proprieties, and has a much large coefficient of thermal expansion (CTE) than typical metals. All these factors make parylene C a much more ideal material for creating large-deflection and low-power underwater actuators than typical MEMS thin film materials such as SiO_2, Si_3N_4, and polysilicon. However, the drawback is that parylene C melts at ~180°C, which is much lower than most common MEMS materials. Hence, a key part of our project was to develop a micro fabrication process to realize the tri-layer thermal actuator structure using parylene C. In the following two sections, the analyses used to estimate the power requirement and temperature-induced bending of the tri-layer parylene actuator are described. The fabrication process, experimental results, and discussion on the frequency response and actuation force of the actuator are then presented in the remaining sections of this paper.

II. Heat Transfer Analysis

Conventional MEMS thermal actuators require relatively high actuation power in aqueous media because much of the input power is dissipated in the form of heat by: 1) conduction to the substrate by the small contact area between the substrate and the actuator (anchor), and 2) convection to the surrounding fluid environment (see Fig. 2). For the anchor, since the conduction path to the substrate is very short, i.e., a few microns of thin film thickness, thus, the heat conduction rate becomes faster and more energy input required. In addition, for actuation in aqueous environment, heat loss to liquid is much greater than that to the air, e.g., the convective heat coefficient of water is ~40 times higher than that of air.

A. Heat Dissipation from the Actuator

By applying the energy balance equation for heat generation and transfer [8] on the platinum metal heater (refer to the equivalent thermal circuit in Fig. 2b) the following equation can be derived:

$$\rho C_p V \frac{\partial T}{\partial t} = I^2 R - \left[\frac{T - T_\infty}{(B_{parylene}/k_{parylene}) + (1/h_{medium})} A_{convection} + \frac{T - T_\infty}{B_{substrate}/k_{substrate}} A_{conduction}\right] \quad (1)$$

where B is the thickness, k is the thermal conductivity, h is the convection heat transfer coefficient, ρ is the density, C_p is the specific heat capacity, A is the effective area for heat loss, and T is the temperature of the heater. Using the above equation, a comparison of heat loss through convection in water and air and conduction through an actuator's anchor for various substrate materials is given in Fig. 3. For this comparison, a small anchor area of 25μm x 12.7μm, parylene top layer thickness of 0.1μm, bottom layer thickness of 0.3μm, and platinum layer thickness of 0.2μm with resistance (measured) of 90Ω were used in the calculation. An ambient temperature of 23°C was also assumed (all other relevant physical parameters are given in Fig. 3).

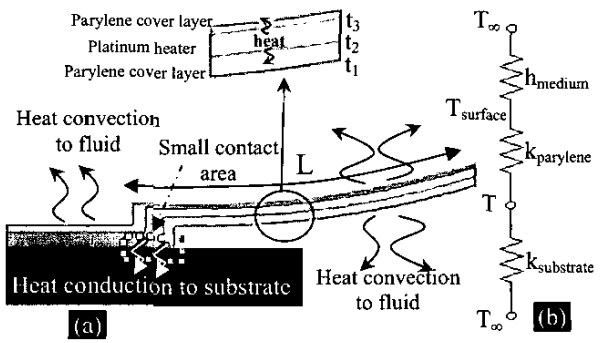

Fig. 2. (a) Illustration showing the cross-section of the thermal actuator; the heat transfer mechanisms of the actuator are also shown. (b) The corresponding equivalent heat-transfer circuit.

As shown, the convection heat loss in water is almost 2 orders of magnitude higher than in air, and therefore, minimizing the convection to aqueous environment is important in minimizing a thermal actuator's energy consumption. By using parylene, which has lower thermal conduction than other standard MEMS insulators, convection loss can be reduced. However, as shown in the figure, the most significant heat loss is by conduction to the Si substrate through the small anchor area. If substrates such as PMMA or glass are used, the conduction heat loss can be significantly reduced, but more complicated fabrication procedures need to be developed in order to process on these substrates. Nevertheless, the graph also indicates that the tri-layer parylene actuators may function at 60°C with total power consumption of <100mW (design space). This power loss is comparable to many reported MEMS underwater actuators while allowing this polymer actuator to operate at a much lower temperature.

B. Thermal Transient Response in Liquid Environment

To estimate the thermal transient response of the actuator, a simple analysis was performed to estimate the required time for it to dissipate the heat generated by its heater. The temperature response of a body initially at temperature T_i immersed in a fluid medium of temperature T_∞ can be solved by the following equation [8]:

$$(T - T_\infty)/(T_i - T_\infty) = \exp[-(hA_s/\rho CV)t] \quad (2)$$

In the above equation ρ, C, and V are the density, specific heat capacity, and volume of the heated material, A_s the convective surface area, and h the

convective heat coefficient. The time constant for this exponential function is:

$$\tau = (1/hA_s)(\rho CV) \tag{3}$$

Hence, with h_{water} ~200W/m^{2}K and h_{air} ~5W/m^{2}K, the time constant for convection in water is ~40 times faster than in air for a given heater. Consequentially, even though the heat loss rate for the actuator is greater in liquid medium than in air, the heat generated by the heater can be dissipated in liquid faster, allowing the actuator to return to its original unactuated position in a shorter time.

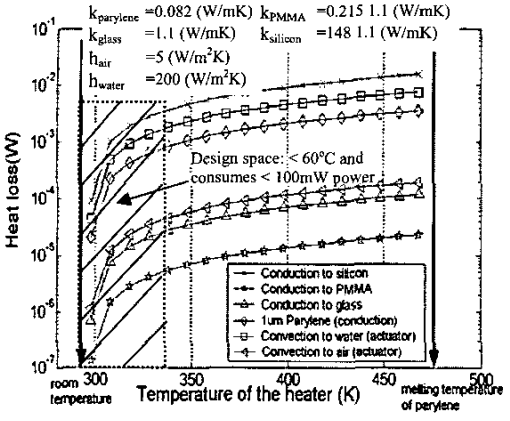

Fig. 3. Comparison of heat loss of the actuator through conduction for various substrate materials and through convection to air and water.

III. Temperature-Induced Deflection for a Tri-Layer Thermal Actuator

The deflection of this polymer-based thermal actuator as a function of temperature can be estimated by a three-layer cantilever beam model. As shown in Fig. 2, the basic actuator structure consists of a middle layer of platinum and top and bottom layers of parylene. When an electrical current is passed through the platinum heater, the entire structure will expand. Due to the difference in CTE between platinum and parylene, different strain will result in the 3 layers, and thereby lead to the curling up of the beam if the thicknesses of the layers are designed appropriately. By considering the interaction of forces and moments between the layers, the bending radius of curvature r due to temperature change ΔT can be calculated by the equations below [8]:

$$r = 1/\left(-\frac{1}{2}AD^{-1}C\right)/\left(-AD^{-1}B\Delta T\right) = g(A,B,C,D)\cdot\frac{1}{\Delta T} \tag{4}$$

where

$$A_{ij} = \left(\sum_{i=1}^{3} E_i I_i\right)^{-1}\left(t_1 + \ldots + t_{j-1} + \frac{t_j}{2}\right) \text{ for } i=1,j=1,2,3 \tag{5}$$

$$B = [\alpha_1 - \alpha_2;\ \alpha_2 - \alpha_3;\ 0] \tag{6}$$

$$C = [t_1 + t_2;\ t_2 + t_3;\ 0] \tag{7}$$

$$D = \left[\frac{1}{E_1 t_1 b_1}\ \ \frac{-1}{E_2 t_2 b_2}\ \ 0;\ \ 0\ \ \frac{1}{E_2 t_2 b_2}\ \ \frac{-1}{E_3 t_3 b_3};1\ \ 1\ \ 1\right] \tag{8}$$

The subscript i is the parameter for the i^{th}-layer. In the above equations, α, t, b, E and I are the CTE, thickness, width, Young's modulus and moment of inertia of the corresponding layers, respectively. The vertical displacement d of the beam can be calculated by the following equation, in which L is the length of the beam (see Fig. 4 for the definitions of r and d):

$$d = r\left[1 - \cos\left(\frac{L}{r}\right)\right] \tag{9}$$

From (4), the bending radius is inversely proportional to temperature change. We set ΔT=40°C as the maximum allowable temperature change in designing the actuators (biological cells may still survive at 40°C above room temperature). In order to minimize the radius of curvature of the tri-layer beam given a ΔT, the function $g(A,B,C,D)$ should be minimized. Since the top and bottom layers are made of the same material, $g(A,B,C,D)$ is inversely proportional to $(\alpha_{heater}-\alpha_{parylene})$. Therefore, one way to optimize the design is to choose a metal that gives larger CTE difference. Another way is to deal with the thickness and width of the beam. For simplicity, we assumed that the widths of the top and bottom layers are the same. By rearranging terms, $g(A,B,C,D)$ can be shown to depend only on t_1, t_{21}, t_{31}, E_{21}, E_{31} and b_{21}, where the ij subscript indicates the ratio of the particular parameter of layer i to j. Since $g(A,B,C,D)$ is an unbounded function, a close form solution for optimizing these variables could not be found. The relationship between the radius of curvature and the thickness ratios is plotted in Fig. 4. It was found that t_{21} and t_{31} should be small in order to give a smaller radius of curvature, but t_1 must also be minimized. Therefore, a numerical analysis was necessary to solve t_1, t_{21} and t_{31} within a certain range (constrained by allowable thin film deposition thickness). After the values of thicknesses were determined, the optimal width ratio b_{21} can be determined by the following equation:

$$b_{21} = sqrt[(1 + 4t_{31} + 12t_{21}t_{31} + 12t_{21}^2 t_{31} + 6t_{31}^2 + 12t_{21}t_{31}^2 + 4t_{31}^3 + t_{31}^4)/E_{21}t_{21}^2] \tag{10}$$

Then, by arbitrarily choosing b_1, b_2 can be determined. By choosing L =2mm, b_1=b_2=100μm, t_1=.1μm, t_2=.2μm, and t_3=.3 μm, then r of 600μm can be achieved at ΔT=40°C (see inset of Fig. 4), which is sufficient to grip a *Danio rerio* follicle as will be shown in the Section V.

IV. Fabrication Process

Several designs of our micro thermal actuators were batch fabricated on a 4-inch silicon wafer using surface micromachining technology. The basic fabrication process flow is shown in Fig. 5. Photoresist (~1.4 μm) is first spun onto the silicon substrate. This layer serves as the sacrificial layer for the actuator. The

first parylene C (~0.3μm) layer is deposited by the PDS 2010 LABCOTER® 2. This polymer layer is patterned by photolithography and etched by oxygen plasma. Next, titanium (~500Å to improve adhesion between platinum and Si) and then platinum (2000Å) are sputtered onto the substrate. These two metal layers are patterned by lift-off at the same time, and serve as the heater for the actuator. A second parylene C layer is then deposited, patterned, and then etched by oxygen plasma. Finally, the structure is sacrificially released by etching the photoresist layer with acetone. Top views of the final patterns of the thermal actuator and the embedded heater are shown in Fig. 5f. Samples of single-finger and multiple-finger grippers fabricated using the described process are shown in Fig. 6, which also shows the effect of residual stress on fabricated actuators.

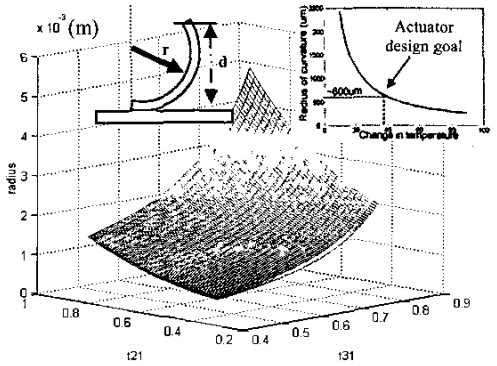

Fig. 4. Relationship between the actuator bending radius and the thickness ratios of the thin film layers making up the actuator. As show in the inset graph, a change of 40°C is required to achieve a gripper closure radius of 600μm.

V. Experimental Results

There are two methods to induce a temperature change in the thermal actuators: 1) passing a current through the resistive heater to increase actuator temperature, and 2) changing the temperature of the medium which surrounds the actuators to heat them up. We have demonstrated that both methods can be used to actuate the parylene-based tri-layer actuators. The results are presented in this section.

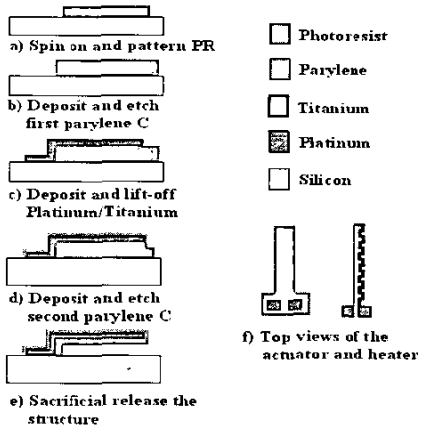

Fig. 5. Fabrication process of the polymer-based thermal actuator.

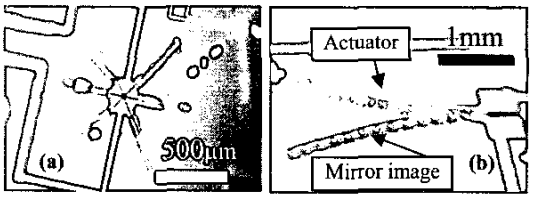

Fig. 6. 3D microscope pictures showing the effects of thin film residual stress and layer thickness variations: (a) the bottom layer parylene is thicker than top layer; (b) the top layer parylene is thicker than bottom layer.

A. Actuation by Applied Voltage

A sequence of motion of a thermal actuator actuated underwater by an applied voltage is shown in Fig. 7. The experiment was carried out in DI water. The resistance of the platinum heater was measured to be ~90Ω. The dimension of the actuator shown is 2mm × 100μm × 0.6μm. The voltage was varied from 0V to 3V within 3 mins to observe the actuator's DC response and obtain its current-voltage (I-V) relationship. It was found that bubbles were generated when the applied voltage was greater than 1.8V (electrolysis); but we have found that by depositing parylene on metal surfaces (i.e., electrical wire and contact pads) exposed to the liquid medium will greatly reduce the number of bubbles that are generated by electrolysis [9].

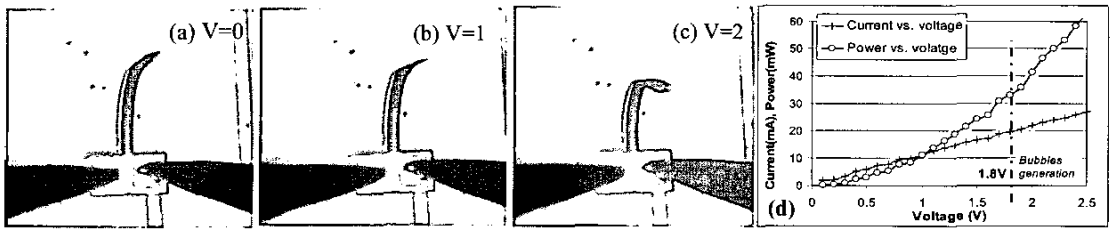

Fig. 7. Sequence of images showing the motion of an underwater actuator driven by applying voltage across the metal heater which is encapsulated by parylene layers. The I-V relationship and power consumption for this actuator is shown in (d). The power consumption of ~60mW at 2.5V input to achieve 90° deflection is predicted by the theoretical results given in Fig. 3.

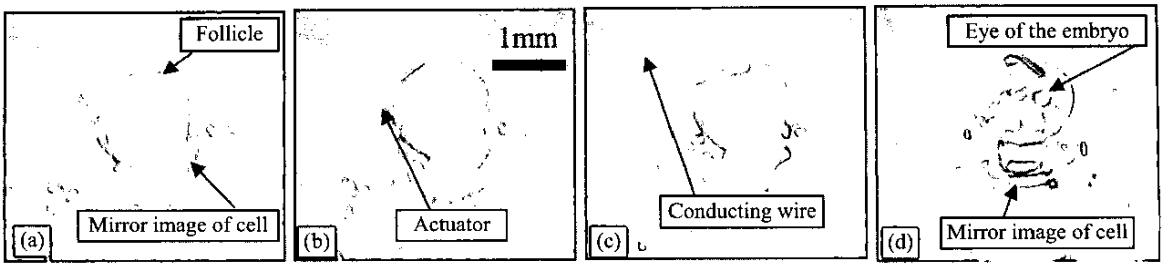

Fig. 8. Sequence of images showing the motion of an underwater actuator by increasing the water medium temperature from 23 to 60°C. We have validated that the Danio rerio follicle is still alive at 60°C, i.e., the embryo inside the membrane was observed to move around after the cell was captured by the actuator. The eye of the embryo can be seen in (d). A MPEG movie file showing the capturing of the cell and the moving embryo can be downloaded from http://www.acae.cuhk.edu.hk/~cmns.

B. Actuation by Heating Fluidic Environment

For actuation by increasing the fluidic medium temperature, the experiment was also carried out in DI water. A sequence of images on the motion of an actuator capturing a follicle using this method is shown in Fig. 8. The temperature of the water was increase from 23°C to around 60°C by a hotplate in 4 mins (see Fig. 9 for experimental setup). *Danio rerio* follicles with diameters ranging from 500μm to 1mm were captured using this actuation method. An advantage of using this actuation technique is that only external thermal energy needs to be applied to the medium, and therefore the actuators can be actuated without electrolysis.

VI. Discussion

Full characterization on the performance of the polymer actuator is underway in our lab. The estimated actuation force and frequency response of this underwater actuator is discussed below.

A. Frequency Response in Liquid Medium

The formula for damped vibrational resonant frequency of a cantilever beam is well known and can be expressed by:

$$\omega_d = \left(\sqrt{1-\zeta^2}\right)\left(\sqrt{[3E(bt^3/12)/L^3]/m}\right) \qquad (11)$$

where the term $((3E(bt^3/12)/L^3)/m)^{1/2}$ is defined as ω_n and is the natural resonant frequency of the beam; E, b, t, and L are the beam parameters as defined in Section III, and m is the mass of the beam. Also, ζ is the damping ratio, which is defined as the ratio between the viscous damping coefficient c_f and the critical damping coefficient $c_o=2m\omega_n$. Experimentally, we have driven the thermal actuators with square wave input and observed that they can be fully actuated up to 3 Hz in liquid medium with full deflection; hence, the viscous damping coefficient is ~0.99 for these actuators base on (11), which implies that damping in liquid environment is significant. The actuators were observed to respond up to 24Hz input, although with diminished tip deflections. More extensive measurements on the frequency response of the actuators are ongoing in our lab.

B. Estimation of Actuation Force

Calibration of gripping force and lifting force of these polymer actuators is difficult by conventional techniques since these actuators have large deflections and are under water. Eventually, we will fabricate different dimensions of silicon blocks to calibrate the force output of the actuators. However, the minimum force output of an actuator must exceed the sum of the fluid drag, gravitational and bending stress forces in order for it to actuate and grip a cell (Fig. 10). Note that in a liquid medium, capillary force (a surface force) between the actuator and the substrate is not a concern because of the absence of air-liquid interface as in the case for actuation in air. So, the following simple analyses were used to give an order of magnitude approximation to the lift force.

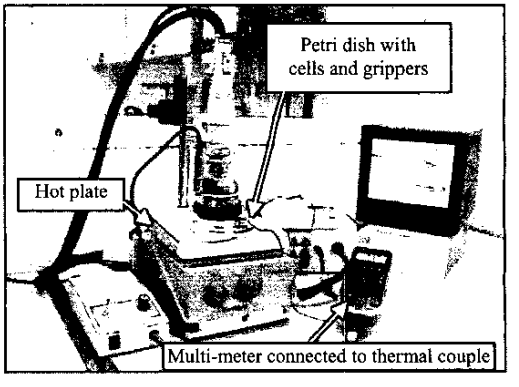

Fig. 9. Experimental setup for actuating the actuators by elevating fluid temperature.

Fluid Drag Force

The Reynolds Number R_e for a body moving in a fluid is calculated as $R_e=\rho U D_e/\mu$. For this problem, ρ is the density of water, U is the velocity of the moving actuator, D_e is actuator characteristic length scale, and μ is the fluid viscosity coefficient. To estimate the velocity of the actuator, we assumed that for a 2mm x 100μm x 0.6μm actuator, the tip will reach 90° within 0.33sec (3Hz actuation). Then, referring to Fig. 10, $U= \pi/2/(0.33)*2=$ 9.5mm/sec. Using a characteristic length of L=2mm, then R_e is <1, which means that the flow is laminar and hence

we can assume the skin friction is negligible, and the only source of drag force is pressure drag (form drag). Then, assuming the worst case scenario where a 1D uniform free-stream flow impinging on a stationary plate, the drag force F_p can be calculated using Bernoulli's Equation:

$$F_P = \rho U^2 A/2 \qquad (12)$$

where $A=bL$, (b is the width and L the length of the actuator) which is the area impinging on the flow, ρ is density of water, and U is the average velocity (9.5mm/sec). Hence, $F_p \sim 13.7$nN.

Weight of the Actuator

The weight of the actuator body F_m is mainly that of the platinum film (0.2μm). Hence, $F_m \sim \rho bLt = 8.4$nN, where ρ is the density of platinum (21.1kg/m^3), and b, L, and t are the actuator parameters as defined in Section III.

Force to Bend the Actuator

Using linear bending beam theory, the actuation force required to deform a beam with a spring constant $k=3E(bt^3/12)/L^3$ by a distance y is approximated by $F_k=ky\sim 0.2$nN. This is the force produced by the beam caused by the thermal induced stress of the beam.

Therefore, the total minimum force output for a 2mm x 100μm x 0.6μm actuator with 3V input (~33mA) is $F_m+F_p+F_k$ and is ~22.3nN based on the above analyses.

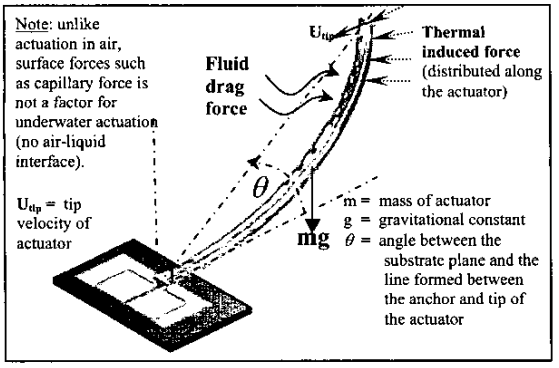

Fig. 10. Illustration showing various forces acting on the actuator.

C. Micro Injection

The actuator was also demonstrated to be able to grip and hold a cell in place during a cell injection process. We have shown that if pipettes with sufficiently small diameters are used, color dyes can be injected into a *Danio rerio* follicle held by the parylene thermal actuators (see Fig. 11).

VII. Conclusion

A novel polymer-based micro robotic actuator has been presented in this paper. We have successfully demonstrated the operation of this actuator in an aqueous environment by two methods: 1) passing a current through the heater to induce resistive heating in the actuator, and 2) changing the temperature of the liquid medium which surrounds the actuator. The voltage required for full deflection is ~3V with power input of ~100mW. We have found that bubbles generated by electrolysis can be eliminated by post parylene deposition on metal surfaces. Moreover, cell grasping of follicle of *Danio rerio* was demonstrated with actuation temperature of ~60°C. For future work, we will control multi-finger microgrippers through a computer and quantitatively evaluate the performance of the microgrippers.

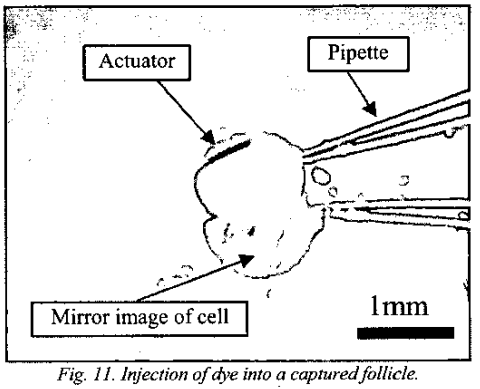

Fig. 11. Injection of dye into a captured follicle.

VIII. Acknowledgement

We thank S. W. Lin, Y. W. Chan, and C. M. Yung from the Department of Molecular Biotechnology at CUHK for their help in sharing and providing valuable information for the *Danio rerio* cells.

IX. References

[1] S. Yu and B. Nelson, "Microrobotic Cell Injection", *Proc. of IEEE Int. Conf. on Robotics and Automation (ICRA 2001)*, Seoul, Korea, 2001, pp. 620-625.

[2] C. C. H. Kwong and W. J. Li, "Fabrication of Nanometric Probe Tips by Sacrificial Boundary Etching", accepted, *The 3rd Biannual Symposium on MEMS (iMEMS 2003)*, Singapore, June 29-July 4 2003.

[3] S. Shoji and M. Esashi, "Microflow devices and systems", *Journal of Micromechanics and Microengineering 4*, 1994, pp. 157-171.

[4] G. Lin, C. J. Kim, S. Konishi and H. Fujita, "Design, fabrication and testing of a C-shape actuator", *Tech. Dig., Transducers'95*, Stockholm, Sweden, 1995, pp. 416-419.

[5] M. Ataka, A. Omodaka, N. Takeshima and H. Fujita, "Fabrication and operation of polyimide bimorph actuators for a ciliary motion system", *Journal of Microelectromechanical Systems*, vol. 2, no. 4, 1993, pp. 146 -150.

[6] E. W. H. Jager, O. Inganas, and I. Lundstrom, "Microrobots for micro-sized objects in aqueous media: potential tools for single-cell manipulation", *Science*, vol. 288, 2000, pp. 2235-2238.

[7] E. Smela, M. Kallenbach, and J. Holdenried, "Electrochemically driven polypyrrole bilayers for moving and positioning bulk micromachined silicon plates", J. of Microelectromechanical Systems, vol. 8, no. 4, 1999, pp. 373-383.

[8] F. P. Ineropera, D. P. DeWitt, *Fundamentals of heat and mass transfer*, John Wiley & Sons, Inc., 1981, pp. 85-86, 212-214.

[9] H. Y. Chan and W. J. Li, "A polymer-based micro thermal actuator for micromanipulations in aqueous environment", *International Journal of Non-linear Sciences and Numerical Simulation*, Vol. 3, Nos. 3-4, 2002, pp. 775-778.